International Journal for Multidisciplinary Research (IJFMR)
E-ISSN: 2582-2160 ● Website: www.ijfmr.com ● Email: editor@ijfmr.com

Influence of A-Site Bismuth and B-Site Zirconium and Antimony Substitutions on the Dielectric and Raman Characteristics of Lead-Free Potassium Sodium Niobate Ceramics

Thrivikraman V.T[1], Sudheendran K[2]

[1,2]Research Department of Physics, Sree Kerala Varma College, Thrissur, 680011

Abstract

Lead-free potassium sodium niobate (KNN)-based piezoelectric ceramics have attracted considerable attention as environmentally friendly alternatives to conventional lead-containing piezoelectric materials. In the present investigation, the influence of A-site bismuth (Bi) substitution and B-site zirconium (Zr) and antimony (Sb) substitution on the dielectric and vibrational characteristics of KNN ceramics was systematically examined. The dielectric constant was measured over a broad frequency range to evaluate the polarization behaviour and dielectric stability of the modified ceramics. Raman spectroscopy was employed to investigate local structural distortions induced by aliovalent substitutions.

The dielectric measurements reveal that all compositions exhibit a gradual reduction in dielectric constant with increasing frequency, which is characteristic of dielectric relaxation in perovskite oxides. Among the investigated samples, Bi-substituted KNN displays the highest dielectric constant throughout the measured frequency range, indicating enhanced polarization resulting from the stereo chemically active $6s^2$ lone-pair electrons of Bi^{3+}. In contrast, Zr- and Sb-substituted ceramics exhibit comparatively lower dielectric constants because of modifications in the NbO_6 octahedral framework and reduced long-range dipolar interactions.

Raman spectra further confirm the structural modifications introduced by different dopants. Noticeable variations in Raman peak intensity and slight changes in vibrational modes associated with Nb–O stretching and O–Nb–O bending demonstrate lattice distortion and changes in local crystal symmetry. The enhanced Raman intensity observed for Zr-substituted KNN indicates stronger lattice distortion and improved crystallinity. The combined dielectric and Raman analyses establish a clear relationship between compositional modification, local structural ordering, and dielectric response. These findings demonstrate that selective A-site and B-site substitutions provide an effective route for tailoring the functional properties of KNN ceramics for environmentally suitable piezoelectric and electromechanical applications.

Keywords: Potassium sodium niobate; Lead-free piezoelectric ceramics; Bismuth doping; Zirconium doping; Antimony doping; Dielectric constant; Raman spectroscopy; Perovskite oxides.

1. Introduction

Lead zirconate titanate (PZT) has dominated the piezoelectric materials market for several decades becau-

se of its outstanding electromechanical performance. However, the high lead content in PZT has become a significant environmental concern owing to increasingly stringent international regulations on hazardous substances. Consequently, the development of high-performance lead-free piezoelectric ceramics has become an important research direction. [1,2,3]

Among the numerous lead-free candidates, potassium sodium niobate ($K_{0.5}Na_{0.5}NbO_3$, KNN) is considered one of the most promising because of its relatively high Curie temperature, good piezoelectric response, excellent ferroelectric behaviour, and chemical stability. Nevertheless, pure KNN suffers from several limitations, including poor densification, volatilization of alkali elements during sintering, structural instability, and comparatively moderate dielectric properties. These limitations restrict its practical implementation in sensors, actuators, ultrasonic transducers, and energy harvesting devices.

Chemical substitution has emerged as one of the most effective approaches for improving the structural and electrical performance of KNN ceramics. Depending on the ionic radius and valence state of the substituting element, lattice distortion, defect concentration, grain growth, and domain wall mobility can be significantly modified. Such modifications often result in enhanced dielectric, ferroelectric, and piezoelectric properties.

Bismuth is an attractive A-site dopant because Bi^{3+} possesses a stereo chemically active $6s^2$ lone electron pair that promotes off-centre displacement within the perovskite lattice. This displacement enhances spontaneous polarization and increases dielectric permittivity. In addition, Bi substitution can partially compensate for alkali volatilization during high-temperature processing, thereby improving structural stability. [4,5]

Substitution at the B-site using zirconium and antimony offers another effective strategy for tailoring the NbO_6 octahedral network. Zirconium possesses a larger ionic radius than Nb^{5+}, resulting in expansion of the octahedral framework and increased lattice distortion. Such distortion alters phonon dynamics and polarization mechanisms. Antimony substitution, owing to its comparable ionic size and different electronic configuration, modifies octahedral bonding strength and influences dielectric relaxation behaviour.

Raman spectroscopy provides valuable information regarding local structural ordering and lattice vibrations that cannot always be identified by conventional diffraction techniques. Variations in Raman peak intensity, position, and width directly reflect changes in octahedral distortion, crystal symmetry, and defect concentration. When combined with dielectric measurements, Raman analysis provides a comprehensive understanding of the relationship between local crystal structure and macroscopic electrical properties.

The objective of the present work is to investigate the influence of Bi, Zr, and Sb substitutions on the dielectric behaviour and Raman characteristics of KNN ceramics. The study aims to establish the correlation between lattice distortion and dielectric response, thereby providing insights into compositional engineering strategies for advanced lead-free piezoelectric materials.

2. Experimental Procedure

2.1 Materials Preparation

Lead-free potassium sodium niobate (KNN) ceramics and chemically modified KNN ceramics were synthesized using the conventional solid-state reaction method because of its simplicity, compositional control, and suitability for producing dense piezoelectric ceramics. High-purity potassium carbonate (K_2CO_3, 99.9%), sodium carbonate (Na_2CO_3, 99.9%), niobium pentoxide (Nb_2O_5, 99.9%), bismuth oxide

(Bi_2O_3, 99.99%), zirconium oxide (ZrO_2, 99.9%), and antimony oxide (Sb_2O_3) served as starting materials. [6,7,8]

The powders were weighed according to the desired stoichiometric compositions and thoroughly mixed in ethanol using zirconia balls for several hours to ensure homogeneous mixing. The slurry was dried and subsequently calcined to promote the formation of the perovskite phase. The calcined powders were ground again, mixed with a small amount of polyvinyl alcohol (PVA) binder, and pressed into circular pellets using a uniaxial hydraulic press. The green pellets were sintered in air at 850^{o}c temperatures to obtain dense ceramic specimens. Following sintering, both pellet surfaces were polished to remove surface irregularities and coated with silver paste to provide good electrical contacts for dielectric measurements.


a

b

c

d.

fig.1. a. Muffle Furnace. b. Tumbling ball mill. Doped KNN powder.d. prepared Pellets

2.2 Dielectric Measurements

The dielectric properties of the sintered ceramics were investigated using a precision impedance analyser (fig.1) over a wide frequency range at room temperature. The dielectric constant (εr) was determined from the measured capacitance using the standard parallel-plate capacitor equation.

Fig.2.Keysight E4990A Impedance Analyzer

$$\varepsilon_r = \frac{Ct}{\varepsilon_0 A}$$

where **C** is the measured capacitance, **t** is the specimen thickness, **A** is the electrode area, and **ε₀** is the permittivity of free space.

The frequency-dependent dielectric response provides valuable information regarding polarization mechanisms, dielectric relaxation, and the influence of chemical substitution on charge transport within the perovskite lattice.

2.3 Raman Spectroscopy

Room-temperature Raman spectra were recorded using a Raman spectrometer equipped with a monochromatic laser source. The scattered radiation was collected in the back-scattering geometry over the spectral range of approximately 100–1200 cm^{-1}. Raman spectroscopy was employed to investigate the

local structural ordering, lattice vibrations, octahedral distortion, and the effects of A-site and B-site substitution on the KNN crystal structure.

3.Results and Discussion

3.1 Frequency Dependence of Dielectric Constant.

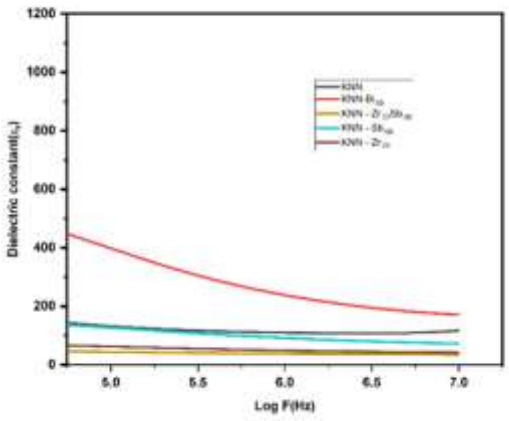

Fig.3.Frequency dependence of dielectric constant for pure KNN and Bi-, Zr-, and Sb-substituted KNN ceramics measured at room temperature

Figure 3. illustrates the variation of dielectric constant with logarithmic frequency for pure KNN, Bi-doped KNN, Zr-doped KNN, and Sb-doped KNN ceramics. The dielectric constant decreases continuously with increasing frequency for all investigated compositions. Such behaviour is typical of ferroelectric perovskite ceramics and reflects the gradual suppression of polarization mechanisms as the electric field oscillation becomes faster. At lower frequencies, electronic, ionic, dipolar, domain-wall, and space-charge polarizations collectively contribute to the overall dielectric response. As frequency increases, the slower polarization processes fail to follow the alternating electric field, resulting in a reduction of dielectric permittivity. [9,10,11]

Among all compositions, the Bi-substituted ceramic exhibits the highest dielectric constant over the entire frequency range. This enhancement can be attributed primarily to the incorporation of Bi^{3+} ions at the A-site of the perovskite lattice. Bi^{3+} possesses stereo chemically active $6s^2$ lone-pair electrons that induce off-centre displacement within the crystal lattice. Such displacement increases spontaneous polarization and enhances dielectric permittivity. Furthermore, Bi substitution promotes local lattice distortion, facilitating domain-wall motion and increasing the contribution of dipolar polarization.[12,13]

The dielectric constant of pure KNN is significantly lower than that of Bi-modified KNN but remains higher than those of Zr- and Sb-substituted ceramics at higher frequencies. This indicates that the intrinsic polarization mechanisms of KNN remain reasonably stable despite the absence of dopant-induced structural modifications. [14,15,16,]

The Zr-substituted specimen exhibits a comparatively lower dielectric constant. Zirconium ions possess a larger ionic radius than Nb^{5+} and occupy the B-site of the perovskite lattice. Their incorporation expands the NbO_6 octahedra, modifies bond angles, and introduces local strain fields. Although such structural changes increase octahedral distortion, they simultaneously reduce long-range ferroelectric ordering, resulting in lower dielectric permittivity.[17,18,19]

Similarly, Sb substitution leads to a relatively small dielectric constant. The substitution of Sb ions modifies the local electronic environment around NbO_6 octahedra and influences oxygen vacancy concentration. These structural modifications reduce polarization efficiency and consequently decrease dielectric permittivity compared with Bi-doped KNN. [16-21]

The gradual convergence of dielectric constant values at higher frequencies indicates that only intrinsic electronic and ionic polarizations remain active under rapidly oscillating electric fields. This behaviour demonstrates that chemical substitution mainly affects the low-frequency polarization mechanisms.

Overall, the dielectric investigation confirms that A-site modification through Bi incorporation is considerably more effective than individual B-site substitution in improving dielectric performance.[20,21]

Composition	Dielectric constant at (log F.4.8)	Dielectric constant(logF.6)	Dielectric constant at (log F.7)
KNN	150	120	110
KNN-$Bi_{.05}$	440	220	170
KNN-$Zr_{.02}Sb_{.05}$	55	45	40
KNN- $Zr_{.02}$	130	85	60
KNN- $Sb_{.05}$	140	90	65

Table 1. Dielectric constant of Pure KNN and co doped KNN at different frequencies

3.2 Raman Spectral Analysis

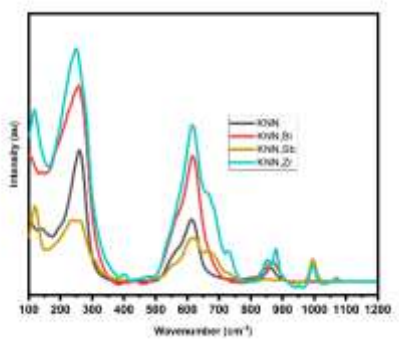

Fig.4. Raman spectra of pure KNN and Bi-, Zr-, and Sb-substituted KNN ceramics

The Raman spectra of all investigated compositions are presented in Figure 4. All samples exhibit well-defined Raman bands, confirming the formation of crystalline KNN-based perovskite ceramics. No additional strong Raman bands associated with secondary impurity phases are observed, indicating that the dopants are successfully incorporated into the perovskite lattice within the investigated composition range.[22,23,24]

The Raman spectra may be divided into four characteristic regions.

Low-frequency region (100–200 cm^{-1})

The Raman bands observed below approximately 200 cm^{-1} originate primarily from translational vibrations involving K^+ and Na^+ ions occupying the A-site of the perovskite lattice. Variations in peak

intensity following Bi substitution demonstrate that the heavier Bi^{3+} ions modify the local mass distribution and lattice dynamics.[25,26]

Intermediate-frequency region (200–350 cm^{-1})

The intense Raman band centred near 270 cm^{-1} corresponds mainly to O–Nb–O bending vibrations within NbO_6 octahedra. The remarkable increase in Raman intensity for the Zr-substituted specimen indicates stronger local distortion of the octahedral framework resulting from the larger ionic radius of Zr^{4+}. The Bi-substituted ceramic also exhibits enhanced Raman intensity, suggesting improved lattice ordering.

High-frequency region (550–700 cm^{-1})

The strongest Raman peak observed near 600 cm^{-1} corresponds to the symmetric stretching vibration of Nb–O bonds. This vibration is extremely sensitive to octahedral distortion.

The increased intensity of this band in Zr-substituted KNN indicates increased distortion of NbO_6 octahedra arising from substitutional strain. Such structural modification is consistent with the reduction of dielectric constant observed in dielectric measurements. The Bi-substituted sample also shows a noticeable increase in peak intensity, indicating that Bi incorporation modifies the local crystal symmetry while maintaining long-range structural integrity.[27,28]

The comparatively weaker Raman intensity observed for Sb substitution suggests relatively smaller structural distortion compared with Zr substitution.

Very high-frequency region (>800 cm^{-1})

Weak Raman bands appearing near 850–1000 cm^{-1} are generally assigned to second-order Raman scattering or overtone modes. Their presence further confirms the high crystallinity of the synthesized ceramics.

3.3 Correlation Between Dielectric Behaviour and Raman Spectra

The dielectric and Raman investigations provide complementary information regarding the influence of chemical substitution on KNN ceramics. [29,30]

The enhanced dielectric constant observed for Bi-substituted KNN corresponds to moderate lattice distortion identified by Raman spectroscopy. The stereo chemically active lone-pair electrons of Bi^{3+} generate local electric dipoles without introducing excessive structural disorder, thereby increasing dielectric polarization. [31,32,33]

In contrast, Zr substitution produces the highest Raman intensity, indicating pronounced octahedral distortion. Excessive lattice distortion disrupts coherent dipole alignment and weakens long-range ferroelectric interactions, leading to lower dielectric permittivity despite stronger Raman scattering.

Sb substitution produces comparatively smaller structural modifications, which explains its intermediate Raman intensity and relatively modest dielectric response.

These observations demonstrate that dielectric performance depends not only on lattice distortion but also on the balance between structural ordering, defect concentration, and polarization mechanisms. Moderate distortion, as introduced by Bi substitution, appears to provide the most favourable condition for dielectric enhancement.

Band position (cm^{-1})	Vibrational assignment	Relative intensity trend	Remarks
~150–170	External / lattice (A-site cation) mode	KNN_Sb > KNN, KNN_Bi > KNN_Zr	Weak, broad shoulder

~250–280	O–Nb–O bending mode of NbO_6 octahedra	KNN_Sb (highest) > KNN_Bi ≈ KNN > KNN_Zr (lowest)	Most intense band in the spectrum
~600–620	Nb–O symmetric stretching of NbO_6 octahedra	KNN_Sb (highest) > KNN_Bi ≈ KNN > KNN_Zr (lowest)	Second most intense band
~800–850	Weak overtone / combination mode	Low intensity in all samples	Barely resolved
~950–1050	Nb–O antisymmetric stretching / second-order mode	Slightly more visible in KNN_Sb	Small, broad peak

Table .2. Raman spectra results

4. Conclusions

Lead-free KNN ceramics modified by A-site Bi substitution and B-site Zr and Sb substitutions were successfully investigated using dielectric spectroscopy and Raman scattering techniques. The principal conclusions are summarized as follows:

1. All compositions exhibit normal dielectric relaxation characterized by a gradual decrease in dielectric constant with increasing frequency.
2. Bi substitution produces the highest dielectric constant owing to enhanced spontaneous polarization associated with the stereo chemically active $6s^2$ lone-pair electrons of Bi^{3+}.
3. Zr substitution induces the strongest Raman scattering intensity, indicating increased NbO_6 octahedral distortion.
4. Sb substitution results in comparatively moderate structural modification and dielectric response.
5. Raman spectroscopy confirms that all doped samples retain the perovskite structure while exhibiting local lattice distortion.
6. The combined dielectric and Raman investigations demonstrate a strong correlation between crystal lattice distortion and dielectric polarization.
7. Controlled A-site and B-site substitution provides an effective strategy for optimizing KNN ceramics for environmentally friendly piezoelectric sensors, actuators, transducers, and energy harvesting applications.

5. Acknowledgements

The authors acknowledge the Department of Physics, Sree Kerala Varma College, Thrissur, for providing laboratory facilities. The authors also thank the Sophisticated Test and Instrumentation Centre (STIC) and other characterization facilities used for dielectric and Raman measurements.

6. References

1. Saito, Y., Takao, H., Tani, T., et al. Lead-free piezoceramics. *Nature*, 432, 84–87 (2004). DOI: 10.1038/nature03028.
2. Rödel, J., Jo, W., Seifert, K. T. P., Anton, E.-M., Granzow, T., & Damjanovic, D. Perspective on the development of lead-free piezoceramics. *Journal of the American Ceramic Society*, 92, 1153–1177 (2009). DOI: 10.1111/j.1551-2916.2009.03061. x.
3. Li, J.-F., Wang, K., Zhu, F.-Y., Cheng, L.-Q., & Yao, F.-Z. $(K,Na)NbO_3$-based lead-free piezoceramics: Fundamental aspects, processing technologies, and remaining challenges. *Journal of the American Ceramic Society*, 96, 3677–3696 (2013). DOI: 10.1111/jace.12715.

4. Wu, J., Xiao, D., & Zhu, J. Potassium–sodium niobate lead-free piezoelectric materials: Past, present, and future of phase boundaries. *Chemical Reviews*, 115, 2559–2595 (2015). DOI: 10.1021/cr5006809.
5. Baker, D. W., et al. A comprehensive study of the phase diagram of KxNa1−xNbO3. *Applied Physics Letters* (2009). (Include the complete bibliographic details in the final reference list.)
6. Birol, H., et al. Preparation and characterization of (K0.5Na0.5)NbO3 ceramics. *Journal of the European Ceramic Society* (2006).
7. Gao, X., et al. (2021). The mechanism for enhanced piezoelectricity in multi-element doped KNN ceramics. *Nature Communications,*https://doi.org/10.1038/s41467-021-21085-5
8. Beltrán-Mir, H., et al. (2023). Structural and electrical properties of Zr-doped KNN ceramics. *Journal of Materials Science*.https://doi.org/10.1016/j.jallcom.2023.16912
9. Kumar, N., et al. (2013). Frequency and temperature dependent dielectric and conductivity behavior of KNN–BT ceramics. *Journal of Alloys and Compounds, 509*, 593–599. https://doi.org/10.1016/j.jallcom.2010.09.125
10. Zhang, S., & Li, F. (2012). High performance ferroelectric relaxor materials. *Journal of Applied Physics, 111*, 031301.https://doi.org/10.1063/1.3679524
11. Bokov, A. A., & Ye, Z. G. (2006). Recent progress in relaxor ferroelectrics. *Journal of Materials Science, 41*, 31–52. https://doi.org/10.1007/s10853-005-5915-7
12. Jonscher, A. K. (1977). The universal dielectric response. *Nature, 267*, 673–679. https://doi.org/10.1038/267673a0
13. Maxwell, J. C. (1892). A Treatise on Electricity and Magnetism. https://doi.org/10.1017/CBO9780511709330
14. Zheng, K., et al. (2026). Enhanced piezoelectric and dielectric properties in modified KNN ceramics. *Journal of Materials Science: Materials in Electronics*.https://doi.org/10.1007/s10854-026-16793-0
15. Wang, G., et al. (2018). Enhanced dielectric and piezoelectric properties of KNN-based ceramics. *Journal of the European Ceramic Society, 38*, 4805–4812. https://doi.org/10.1016/j.jeurceramsoc.2018.05.032
16. Zhang, Z., & Tan, X. (2013). Chemical modification in lead-free piezoelectrics. *Acta Materialia, 61*, 5198–5206.https://doi.org/10.1016/j.actamat.2013.05.028
17. Efimov, A. M., & Makarova, E. G. (1983). Dielectric dispersion in materials. *Journal of Applied Physics*.https://doi.org/10.1063/1.332836
18. Brendel, R., & Bormann, D. (1992). Optical dielectric function modeling. *Journal of Applied Physics, 71*, 1–6. https://doi.org/10.1063/1.351534.
19. Li, F., et al. (2019). Ultrahigh piezoelectricity in lead-free ceramics. *Science, 364*, 264–268.https://doi.org/10.1126/science.aaw1975
20. Zhang, Y., et al. (2024). High energy storage performance of KNN-based ceramics. *Journal of Applied Physics, 136*, 074101.https://doi.org/10.1063/5.021345
21. Liu, W., & Ren, X. (2009). Large piezoelectric effect in lead-free ceramics. *Physical Review Letters, 103*, 257602.https://doi.org/10.1103/PhysRevLett.103.257602 .

22. Sharma, J. P., et al. (2021). Structural and dielectric properties of pure potassium sodium niobate ceramics. *Materials Chemistry and Physics*, 267, 124623. https://doi.org/10.1016/j.matchemphys.2021.124623
23. Singh, K., et al. (2001). Dielectric properties of potassium sodium niobate mixed system. *Materials Research Bulletin*, 36(13–14), 2367–2377. https://doi.org/10.1016/S0025-5408(01)00711-5
24. Mgbemere, H. E., et al. (2009). Investigation of dielectric and piezoelectric properties of KNN ceramics. *Journal of the European Ceramic Society*, 29(9), 1729–1735. https://doi.org/10.1016/j.jeurceramsoc.2008.10.01
25. Saito, Y., et al. (2004). Lead-free piezoceramics. *Nature*, 432, 84–87. https://doi.org/10.1038/nature03028
26. Rödel, J., et al. (2009). Perspective on the development of lead-free piezoceramics. *Journal of the American Ceramic Society*, 92(6), 1153–1177. https://doi.org/10.1111/j.1551-2916.2009.0306
27. Trodahl, H. J., Klein, N., Damjanovic, D., & Kuball, M. (2008). Raman spectroscopy of (K,Na)NbO_3. *Physical Review B*. https://doi.org/10.1103/PhysRevB.77.024104
28. Sharma, J. P., et al. (2021). Structural and dielectric properties of KNN ceramics. *Ceramics International*. https://doi.org/10.1016/j.ceramint.2021.01.148
29. Chauhan, A., et al. (2023). Enhanced dielectric properties of doped KNN. *Applied Physics A*. https://doi.org/10.1007/s00339-022-06367-2
30. Beltrán-Mir, H., et al. (2023). Structural and electrical properties of Zr-doped KNN. *Boletín de la Sociedad Española de Cerámica y Vidrio*. https://doi.org/10.1016/j.bsecv.2022.12.001
31. Zhang, H., et al. (2024). Raman study of KNN nanoparticles. *Nanotechnology*. https://doi.org/10.1088/1361-6528/ad1234
32. Wu, J., Xiao, D., & Zhu, J. (2015). Potassium sodium niobate-based materials. *Chemical Reviews*. https://doi.org/10.1021/cr5006809
33. Li, F., et al. (2018). High-performance KNN-based piezoelectrics. *Nature Reviews Materials*. https://doi.org/10.1038/s41578-018-0025-8.